

# Effect of Vinylacetate Content on Crystallinity and Second-Order Transitions in Ethylene–Vinylacetate Copolymers

M. BROGLY, M. NARDIN, J. SCHULTZ

CNRS–Institut de Chimie des Surfaces et Interfaces (ICSI), 15, rue Jean Starcky,  
B.P. 2478-F-68057 Mulhouse Cedex, France

Received 7 May 1996; accepted 2 October 1996

**ABSTRACT:** Thermal characteristics of ethylene–vinylacetate (EVA) copolymers having vinylacetate contents ranging from 5 to 40 w/w % are studied by differential scanning calorimetry. It is first shown that EVA copolymers having a vinylacetate content lower than 30 w/w % obey the Flory and Burfield theories of copolymer crystallisation. The minimum sequence length of CH<sub>2</sub> ethylenic entities required to participate in a crystalline lamella is also deduced. One can conclude that EVA copolymers represent cases of “total exclusion” of the noncrystallizable comonomer. Moreover, it is observed that when the vinylacetate content is increased, the relative quantity of polyethylene amorphous phase increases and the degree of crystallinity decreases; whereas the  $\beta$  transition temperature of a characteristic-oriented amorphous phase is kept constant. A phase model of ethylene–vinylacetate copolymers, based on an enrichment process of the interlamellar amorphous phase by polyethylene segments originating from the crystalline phase, at increasing vinylacetate content, is proposed. © 1997 John Wiley & Sons, Inc. *J Appl Polym Sci* **64**: 1903–1912, 1997

**Key words:** ethylene–vinylacetate copolymer; glass transition;  $\beta$  transition; crystallinity; differential scanning calorimetry

## INTRODUCTION

Poly (ethylene–vinylacetate) copolymers (EVA), having vinylacetate (VA) content ranging from 5 to 40 w/w %, are the basic components of hot-melt and pressure-sensitive adhesives. They represent up to 80% of the total ethylene–vinylacetate copolymer market in Europe, and the hot-melt adhesives world market is one of the most rapidly growing in the domain of adhesives. Such a situation results from major thermodynamic and rheological advantages of EVA copolymers allowing compatibility, fast processing, and automation. However, EVA copolymers are multiphase materials; and relationships between their structural, physical, and thermal properties are not clearly

established at the present time. In this article, EVA copolymers (in the range of 5–40 w/w % VA) are systematically studied by differential scanning calorimetry (DSC). Second-order thermal transitions are measured and related to non-classical thermal behavior of amorphous phases in such copolymers. Comparisons between experimental and theoretical values of the magnitude of the transition enable us to discuss results in terms of a  $\beta$  transition. The melting temperature and the associated melting enthalpy are measured in order to determine the relevance of the classical copolymer theories to EVA copolymers. These results will allow us to highlight the dependence between crystallinity and  $\beta$  transition.

## EXPERIMENTAL

Six EVA copolymers (Elf-Atochem, France), having VA contents of 5, 9, 14, 18, 28, and 40 w/w

Correspondence to: M. Brogly.

© 1997 John Wiley & Sons, Inc. CCC 0021-8995/97/101903-10

**Table I** Structural Characteristics of EVA Copolymers

%VA (w/w)	%VA (mol)	$M_w$ (g/mol)	$M_n$ (g/mol)	$I_p$ (polydispersity)	Branching Content
5	1.7	64770	18140	3.6	1.4%
10	3.5	60340	16440	3.7	1.2%
14	5	58900	17380	3.4	1.0%
18.5	6.9	56600	17360	3.3	0.7%
27.2	10.8	43810	13700	3.2	0.75%
41.7	18.9	44720	15500	2.9	0.45%

% were studied. The structural characteristics of these copolymers, i.e., weight and number-average molecular weights ( $M_w$  and  $M_n$ ) and polydispersity ( $I_p$ ) were determined by gel permeation chromatography (GPC). The aliphatic branching content was determined by  $^{13}\text{C}$  nuclear magnetic resonance (NMR) relative to one hundred carbon atoms of the hydrocarbon backbone. All these structural characteristics are gathered in Table I. Moreover, the copolymers studied here strictly follow Bernoulli's statistical model of copolymer sequences distribution. Theoretical values of ethylene–vinylacetate–ethylene (EVE) and vinylacetate–vinylacetate–ethylene (VVE) sequence distributions fit experimental values (2% error). As an example, for the EVA copolymer having a vinylacetate content of 28 w/w %, the EVE statistical distributions are equal to 0.79 and 0.78 for the theoretical and experimental values, respectively. Therefore, we can consider that the polymers studied here are purely statistical. One can also notice that the aliphatic branching content logically decreases as the vinylacetate content increases. The thermal characteristics, i.e., glass transition temperature  $T_g$ ,  $\beta$  transition temperature  $T_\beta$ , melting temperature  $T_f$ , and degree of crystallinity  $\chi$  were determined by DSC on a Mettler TA 3000 apparatus. Each sample was first heated up rapidly to 423 K and then isothermally kept at this temperature for 10 min in order to conceal its thermal history. Thus, each sample was cooled down from 423 to 123 K at a cooling rate of 0.1 K min $^{-1}$ . After a 10 minute isotherm at 123 K, a second heating thermogram was recorded at a heating rate of 10 K min $^{-1}$ , revealing the  $\beta$  transition temperature, the glass transition temperature, the melting temperature, and the melting enthalpy.

Considering, at equilibrium, that VA comonomer units are not able to participate in crystalline lattice (i.e., the crystalline phase in the copolymers results from pure polyethylene co-units due

to total exclusion of VA comonomer units), it is assumed that the degree of crystallinity  $\chi$  can be calculated according to Flory's theory of copolymer crystallization.<sup>1</sup> Flory proposed the following equilibrium melting temperature evolution law for copolymers, adapted to ethylene copolymers:

$$\frac{1}{T_f} - \frac{1}{T_f^0} = - \frac{R}{\Delta H_{PE}} \ln F_{PE} \quad (1)$$

where  $T_f$  is the EVA melting temperature at thermodynamic equilibrium;  $T_f^0$ , the pure polyethylene melting temperature at thermodynamic equilibrium;  $R$ , the ideal gas constant;  $\Delta H_{PE}$ , the pure polyethylene crystal melting enthalpy; and  $F_{PE}$ , the crystallizable ethylene molar fraction, given by

$$F_{PE} = 1 - F_{AV} - F_{Br} \quad (2)$$

where  $F_{AV}$  is the VA molar fraction in the EVA copolymer, and  $F_{Br}$  is the branching molar fraction in the EVA copolymer.

When eq. (1) is experimentally verified, Flory expressed the degree of crystallinity  $\chi$  as

$$\chi = (F_{PE})^L \cdot [1 + c_1 \cdot F_{NC} + c_2 \cdot F_{NC}^2] \quad (3)$$

where  $L$  is the minimum crystallizable ethylene sequence length,  $F_{NC}$  is the molar fraction of non-crystallizable entities in EVA, and  $c_1$  and  $c_2$  are experimental constants.

Burfield<sup>2</sup> proposed for low-density linear polyethylene-based copolymers a particular case of Flory's equilibrium generalized theory, as follows:

$$\chi = k' (F_{PE})^L \text{ with } 0.47 < k' < 1 \quad (4)$$

Assuming  $k' = 1$ , Burfield's law suited Flory's law to a first approximation. One must be aware of the fact that eq. (3) represents the maximum

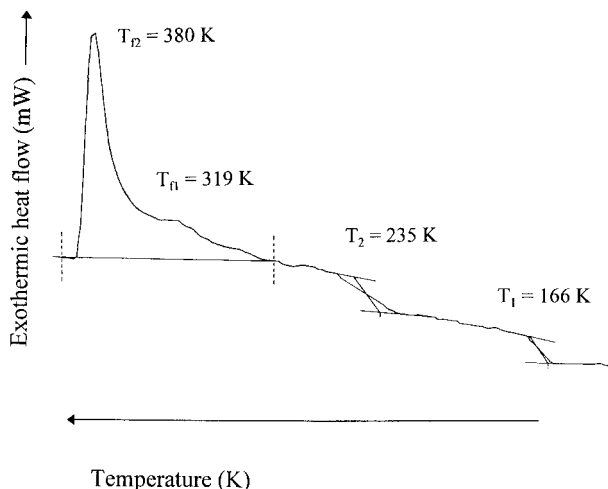


**Figure 1** DSC thermograms of the EVA copolymers for VA contents equal to 9 (a) and 28 (b) w/w %, respectively.

crystalline fraction that can be isothermally obtained in a copolymer having one non-crystallizable comonomer, like VA in the EVA copolymers.

Nevertheless, in order to deduce experimental values of  $k'$  and  $L$ , the degree of crystallinity of EVA copolymers was calculated from the following expression:

$$\chi = \frac{\Delta H}{\Delta H_0} \quad (5)$$

where  $\Delta H$  is the measured melting enthalpy of the polyethylene-enriched phase in EVA copolymers, and  $\Delta H_0$  is the equilibrium melting enthalpy of a pure crystal of linear polyethylene and taken equal<sup>3</sup> to 293 J/g.

Finally, optical microscopical observations of the EVA crystalline entities were performed on thin layers (50  $\mu\text{m}$ ) at room temperature under polarized light by means of a Leitz microscope.

## RESULTS AND DISCUSSION

Figure 1 presents a typical DSC thermogram of EVA copolymers (28 w/w % VA). It shows that such copolymers exhibit two second-order transition temperatures,  $T_1$  and  $T_2$ , for which the onset is located at 166 and 235 K, respectively. The melting process appears rather complex in all cases, indicating that a large continuum of crystal morphologies is involved. Two peaks of unequal broadness are observed on DSC thermograms

whatever the VA content. To a first approximation, we would consider as an assumption that these two peaks are related to the existence of two predominant crystal morphologies. Further calculations would or would not validate such an assumption. Concerning the second-order transitions, the first one,  $T_1$ , is attributed to an amorphous phase A1 of pure polyethylene<sup>4</sup> and will be named  $T_{g1}$  from now on. The second transition,  $T_2$ , which is intermediate between the glass transition temperatures<sup>5</sup> of polyethylene homopolymer ( $\sim 168$  K) and the glass transition of polyvinylacetate ( $\sim 303$  K) homopolymer, has often been identified as a glass transition temperature.<sup>6</sup> Popli<sup>7</sup> has suggested that this transition should be attributed to a  $\beta$  transition relative to a segmental motion that occurs within the interfacial regions associated with the crystallites (in the case of linear polyethylene). Of course, the molecular interpretation of such a  $\beta$  transition will be complicated by the rather complex crystallinity of EVA copolymers. This transition temperature will thus be named  $T_\beta$ . We shall prove further in the study that this  $\beta$  transition depends strongly on the existence of crystalline structures and is probably due to segmental motion in the EVA amorphous phase A2.

It clearly appears in Table II that both glass transition temperature  $T_{g1}$  and  $\beta$  transition temperature  $T_\beta$  are roughly constant whatever the VA content of the copolymer, at least in the range of 5–40 w/w %. This is *a priori* a surprising result, especially for the EVA amorphous phase A2 since the actual VA content of the studied copolymers is a large range (5–40 w/w %). On the contrary, it has been observed that the magnitude of heat variation, defined in terms of specific heat  $\Delta Cp$ , which represents the amount of matter affected by the transitions, depends on the vinylacetate content. Figure 2 shows the variation of  $\Delta Cp_g$  and  $\Delta Cp_\beta$ , associated to  $T_{g1}$  and  $T_\beta$ , respectively, versus the VA content in semilogarithmic scales. A straight line is obtained for the  $\Delta Cp_g$ –VA comonomer units' relationship of the pure polyethylene amorphous phase A1, indicating that the relative quantity of pure polyethylene amorphous phase in EVA copolymers increases with the VA content. This result is consistent and indicates that increasing the VA comonomer content favors the amorphization of the copolymer. On the contrary,  $\Delta Cp_\beta$  linearly decreases in semilogarithmic scales with VA content. Such evolution of the amount of amorphous phases reflects the consequence of crystalline structure growth, which is expected to

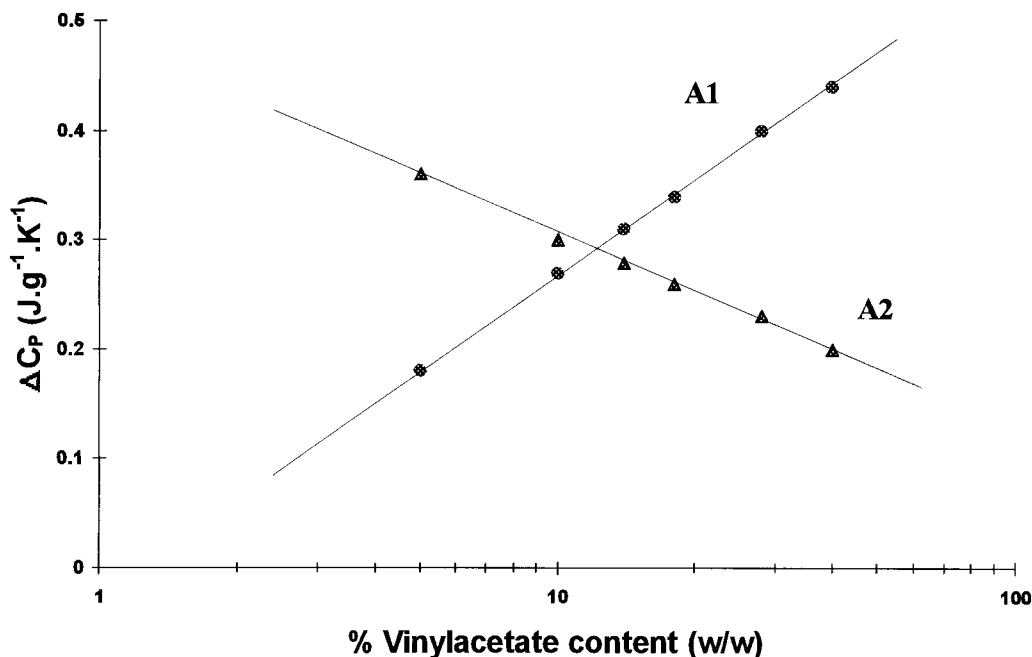
**Table II** Glass Transition Temperature  $T_{g1}$  and  $\beta$  Transition Temperature  $T_{\beta}$  and Their Association Variation of Specific Heat as a Function of VA Content

VA Content (w/w %)	$T_{g1}$ (K)	$\Delta C_{p_g}$ (Jg <sup>-1</sup> K <sup>-1</sup> )	$T_{\beta}$ (K)	$\Delta C_{p_{\beta}}$ (Jg <sup>-1</sup> K <sup>-1</sup> )
5	172	0.18	238	0.36
10	167	0.27	237	0.30
14	166	0.31	237	0.28
18.5	166	0.34	237	0.26
27.2	166	0.40	235	0.23
41.7	166	0.44	239	0.20
Average values	-167 ± 3	—	237 ± 2	—

decrease as the VA content increases; but the explanation of the  $\Delta C_{p_{\beta}}$  behavior implies the analysis of the crystalline structures of EVA copolymers. It may be anticipated that this non-classical amorphous phase would be greatly affected by the development of crystallinity.

Concerning the crystallinity of EVA copolymers, it appears, according to Fig. 1, that this is rather complex, including two major components of different broadness: the first one is called C1 near 319 K (for 28 w/w % VA); the second one is called C2 near approximately 380 K (for 28 w/w % VA). As an assumption, it can be assumed to a first approximation that two types of crystalline structures are involved in EVA copolymers melt-

ing behaviour and exhibit different degrees of perfection of crystalline lamellae and morphologies. Once more, it is evident that these phases are composed of a rather wide distribution of crystals, both in size and morphologies. The lower temperature phase C1 corresponds to a poorly organized structure, whereas the higher temperature phase C2 is closer to that of pure polyethylene. In order to highlight the nature of this latter, the evolution of the reciprocal melting temperature ( $T_f^{-1}$ ) versus the crystallizable ethylene molar fraction  $F_{PE}$  in EVA copolymers is represented in Figure 3. Corresponding data, i.e.,  $F_{AV}$ ,  $F_{Br}$ ,  $F_{PE}$ , and  $T_f$  for crystalline phases C1 and C2 are gathered in Table III. Figure 3 clearly evidences that the high

**Figure 2** Specific heat  $\Delta C_{p_g}$  and  $\Delta C_{p_{\beta}}$ , corresponding to the glass transition of polyethylene A1 and EVA A2 amorphous phases versus VA content.

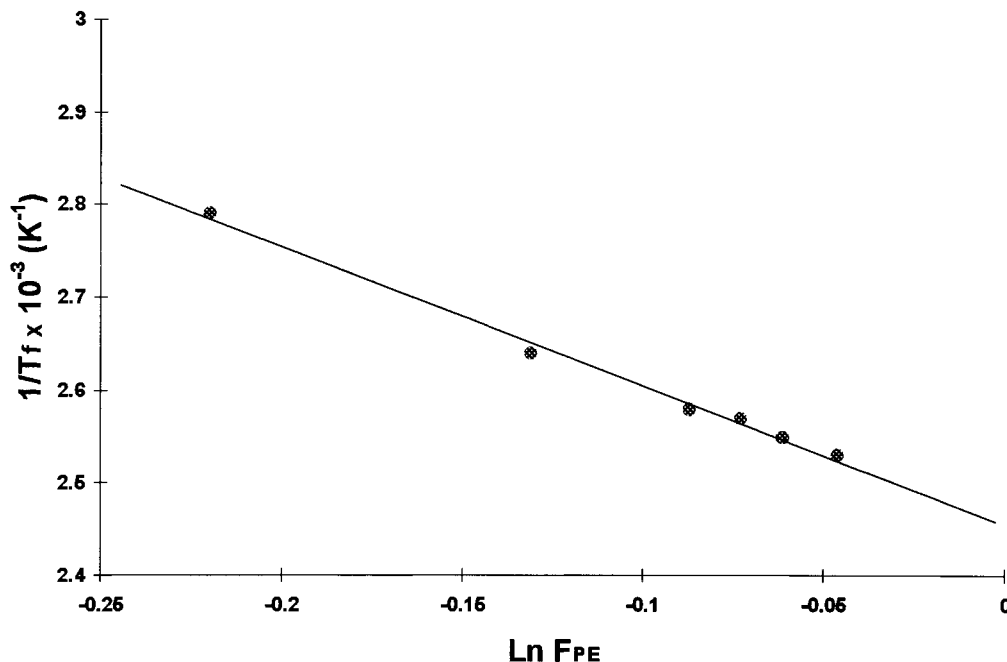


**Figure 3** Crystallizable ethylene molar fraction  $F_{PE}$  versus the reciprocal melting temperature ( $T_f^{-1}$ ) for the highly crystalline C2 phase.

temperature phase C2 for 5 to 28 w/w % VA ranged copolymers follows, to a first approximation, Flory's generalized theory of copolymer crystallization. Nevertheless, it is important to note that we consider that a cooling rate of  $0.1 \text{ K/min}^{-1}$  reflects, to a first approximation, isothermal behaviour. Calculation of both intercept and slope of straight line in Figure 3 leads to the determination of the melting temperature of pure polyethylene crystal at thermodynamic equilibrium,  $T_f^0 = 403 \text{ K}$ , and  $\Delta H_{PE} = 6.98 \text{ J/mol}$  (i.e.,  $249.3 \text{ J/g}$ ), the corresponding melting enthalpy.  $T_f^0$  and  $\Delta H_{PE}$  are in good agreement with the data of Sirota<sup>8</sup> and Aggarval<sup>9</sup> for low branched polyethylene. Then, according to these results, it can be assumed that  $T_f^0$  and  $\Delta H_{PE}$  values obtained for the

C2 phase could be associated with values expected for a pure polyethylene crystal, homostructural in the branching state to ethylene crystallizable sequence length of the EVA copolymers.

On the contrary, the low melting temperature crystalline phase C1 does not follow the theory of copolymer crystallization when VA is increased. The resulting  $T_f^0$  value, equal to  $370 \text{ K}$ , available only for low VA content copolymers ( $<9 \text{ w/w } \%$ ) corresponds to the melting temperature of highly branched polyethylene.<sup>9</sup> As a consequence, the crystalline structure appears to be greatly disorganized. To a first approximation, it is reasonable to assume that both crystalline phases, C1 and C2, could stem from the cumulative effects of different degrees of branching of polyethylene seg-

**Table III** Structural and Experimental Data Corresponding to Flory's<sup>1</sup> Generalized Theory of Copolymer Crystallization

%VA (w/w)	$F_{AV}$	$F_{Br}$	$F_{PE}$	$T_{f1}$ (°C)	$T_{f2}$ (K)
5	0.0168	0.028	0.955	346	395
10	0.0349	0.024	0.941	338	392
14	0.0503	0.020	0.930	335	389
18.5	0.0688	0.014	0.917	331	387
27.2	0.1082	0.015	0.877	319	380
41.7	0.1889	0.009	0.802	315	358

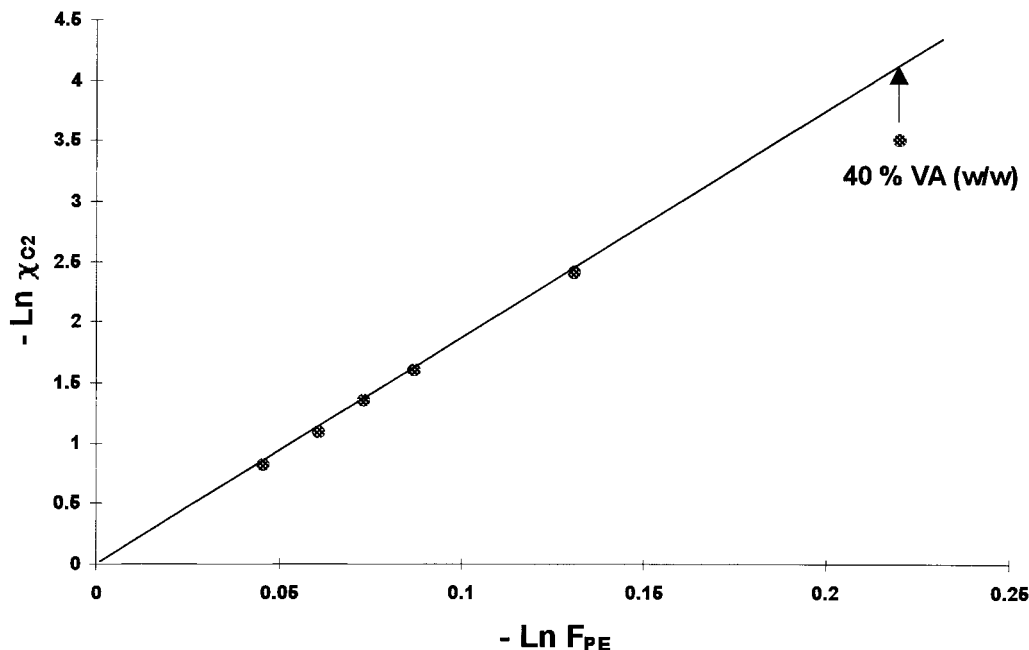


**Figure 4** Crystallizable ethylene molar fraction  $F_{PE}$  versus the crystallinity  $\chi_2$  of the crystalline phase C2.

ments and of various lengths of chain folding in crystals. Moreover, kinetic effects could also be involved: the first crystals formed at high temperature during cooling correspond to the adsorption of low branched polyethylene segments on crystal nuclei. Thus, segments with high branching degrees would be excluded and could only crystallize in a less-organized form (the C1 phase) at the end of the crystallization process.

The degree of crystallinity  $\chi_1$  and  $\chi_2$  of both crystalline phases in EVA copolymers are determined by curve deconvolution of the complex melting peak. At low VA contents, i.e., 5, 9, 14, and 18 w/w %, a straight base line can be drawn on the DSC thermogram, allowing the determination of the melting enthalpies [Fig. 1(a)]. For VA contents in the range of 28–40 w/w %, the  $\beta$  transition zone and the melting process are partly overlapping. Therefore, it is necessary to use a spline function as a base line for the melting peak.

In Figure 4,  $\chi_2$  is plotted versus the molar fraction of crystallizable ethylene co-units in EVA,  $F_{PE}$ , in logarithmic scales, according to Burfield's law that only the C2 phase would obey. One can note that EVA copolymers having a VA content higher than about 30 w/w % do not obey Burfield's crystallinity prediction. This effect can be attributed either to the high vinyl branching content, which induces the exclusion of the resulting ethylene segments from highly organized crystalline

morphologies, or to the difficulty in separating the respective contributions of first- and second-order transition for high VA content copolymers. The results described previously (Fig. 3; Flory's law) tend to confirm the second hypothesis. The straight line obtained in logarithmic scales for the phase C2 of copolymers having VA contents ranging from 5–30 w/w % clearly confirms that branched olefinic chains are excluded from the crystalline lamellae.

Thus, this well-organized polyethylene crystalline structure is very sensitive to the presence of VA and disappears when the VA content is higher than 45 w/w % (20 mol %) in Figure 5. This extrapolated vanishing of the phase C2 can be attributed to steric hindrance phenomena and is strongly associated with the increase of the amorphous and probably oriented EVA amorphous phase responsible for the  $\beta$  transition (Fig. 2).

Equation (4) allows us to calculate  $k'$  and  $L$  from the intercept and the slope of the straight line, respectively, in Figure 4.  $k'$  is found equal to 1.08. This value is not far from the 0.47–1 interval proposed by Burfield for low-density linear polyethylene and reflects the VA comonomer effect. A  $k'$  value greater than unity implies [eq. (3)] that Flory's theory is obeyed and that the molar fraction of non-crystallizable entities has an influence on crystallinity.  $L$  represents the minimum segmental sequence length of ethylene

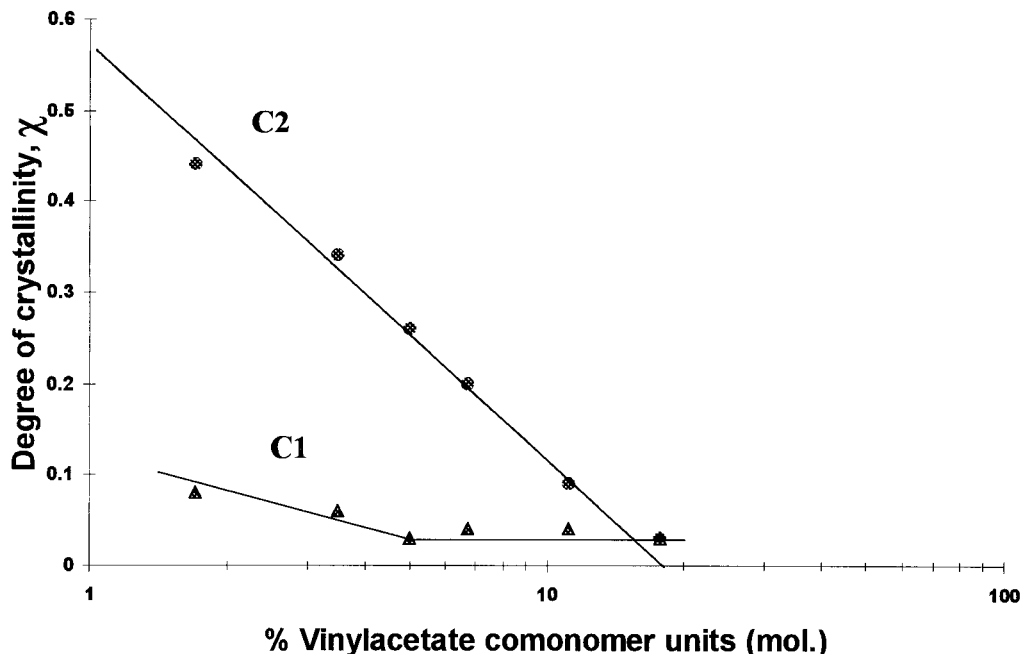


**Figure 5** Degrees of crystallinity  $\chi_1$  and  $\chi_2$  of the less-organized C1 and the well-organized C2 crystalline phases, respectively, versus VA content.

entities that can participate in crystalline lamellae and is found equal to 18.2. This value is fully consistent with the statistical sequence length of seventeen  $\text{CH}_2$  entities between two vinyl branches for a 28 w/w % VA copolymer. This result is of major importance and explains why copolymers having a VA content higher than 30 w/w % do not obey Burfield's prediction. Nielsen<sup>10</sup> confirms our results, proposing a  $L$  value of 25 for 30 w/w % VA EVA copolymers. On the contrary, the crystalline phase C1 remains low but constant (Fig. 5) at a high VA content. This less-organized and degenerated crystalline structure (high branching and folding content) should be regarded as a continuum displayed on a large temperature scale.

These results on the crystalline behavior of EVA copolymer allow us to propose the following hypothesis to explain the non-classical behaviour of the specific heats observed in Figure 2. The knowledge of both the degree of crystallinity of EVA copolymers and the specific heat variation at the second order transition temperature for polyvinylacetate [ $\Delta C_p(\text{PVAc}) = 34.5 \text{ J/mol}^{-1}/\text{K}^{-1}$ ] and polyethylene [ $\Delta C_p(\text{PE}) = 20 \text{ J/mol}^{-1}/\text{K}^{-1}$ ] homopolymers allows us to calculate the EVA theoretical  $\Delta C_p$  value according to

$$\Delta C_p = (1 - \chi) \cdot \Phi_{PE} \cdot \Delta C_p(\text{PE}) + (1 - \Phi_{PE}) \cdot \Delta C_p(\text{PVAc}) \quad (6)$$

where  $\Phi_{PE}$  represents the molar fraction of ethylene comonomers in EVA. We show in Figure 6 the comparison of experimental and calculated specific heat  $\Delta C_p$  values versus VA comonomer units content. Both curves exhibit similar evolution in semilogarithmic scales. However, experimental values are always greater than calculated ones. This difference means that the thermal response of the amorphous phases in EVA copolymers does not follow a classical additive law as proposed in eq. (6). In other words, this tends to prove that the amorphous phase A2 behaves as an original amorphous phase associated with a characteristic specific heat variation. This hypothesis is fully supported by the fact that the  $\Delta C_{p_g}$  and  $\Delta C_{p_\beta}$  depend clearly on the crystallizable ethylene molar fraction. Moreover, it is well known that a significant proportion of the flux of chains that emanate from the basal plane of crystalline lamellae are highly constrained. At the transition temperature  $T_\beta$ , severe conformational differences between the crystalline and the amorphous liquid-like states exist. Therefore, these macromolecular segments relaxations are associated with high energy absorption, i.e., a high  $\Delta C_p$  value. We propose to attribute the difference in Figure 6 to an interlamellar interphasial amorphous phase. This phase is revealed through the  $\beta$  transition temperature.

Finally, Figure 7 presents two optical micro-

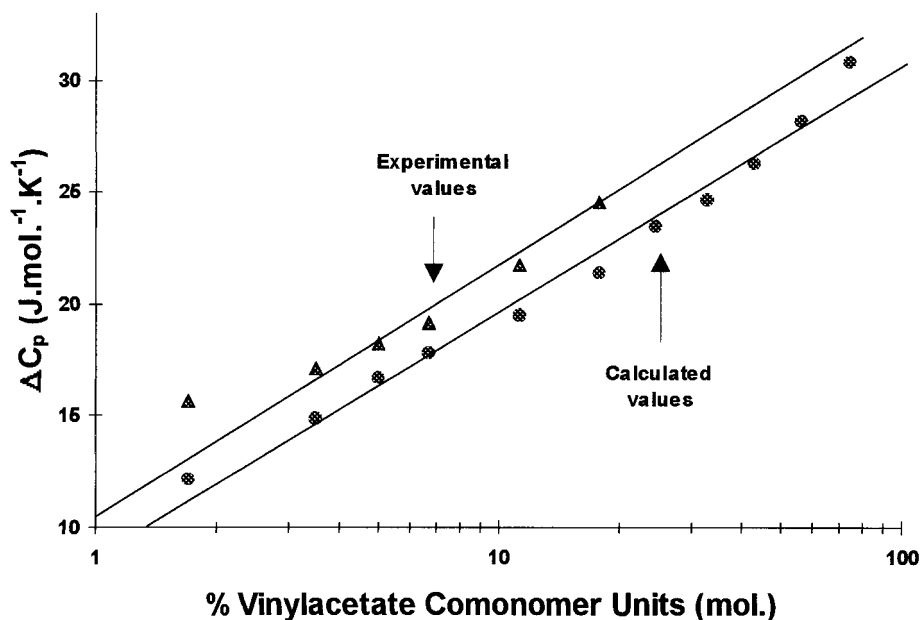


**Figure 6** Comparison of experimental and calculated specific heat  $\Delta C_p$  versus VA comonomer units content.

graphs in polarized light of EVA copolymers at 5 w/w % [Fig. 7(a)] and 28 w/w % [Fig. 7(b)] of VA. It is clear that the size of the crystallites decreases, whereas their number increases, with increasing content of VA. As a consequence, both the amount of interphasial amorphous phase and the crystalline entities decrease with VA content.

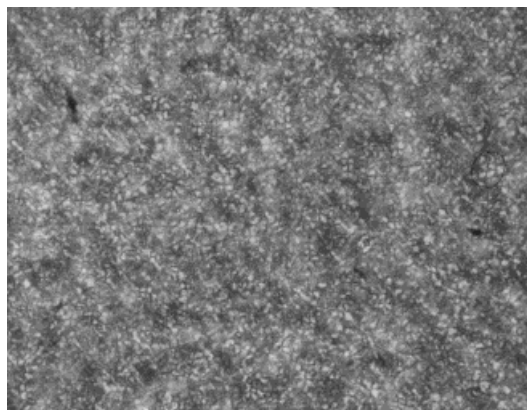
#### Tentative Model of EVA Phase Morphology

From all these results, it is possible to propose a general scheme for the phase morphology of EVA

copolymers. The main fact observed during this study is that the  $\beta$  transition temperature  $T_\beta$  of the amorphous copolymer phase is kept constant, whatever the VA content, ranging from 5 to 40 w/w %. Taking into account the two other major results previously obtained when the VA content increases, i.e., the content decrease of the well-organized crystalline phase C2 and the content increase of the amorphous polyethylene phase A1, it can be assumed that a dilution process of the amorphous copolymer phase A2 by polyethylene segments originating from pure polyethylene la-



(a)



(b)

**Figure 7** Optical micrographs of EVA copolymers in polarized light for VA contents equal to 5 (a) and 28 (b) w/w %, respectively.



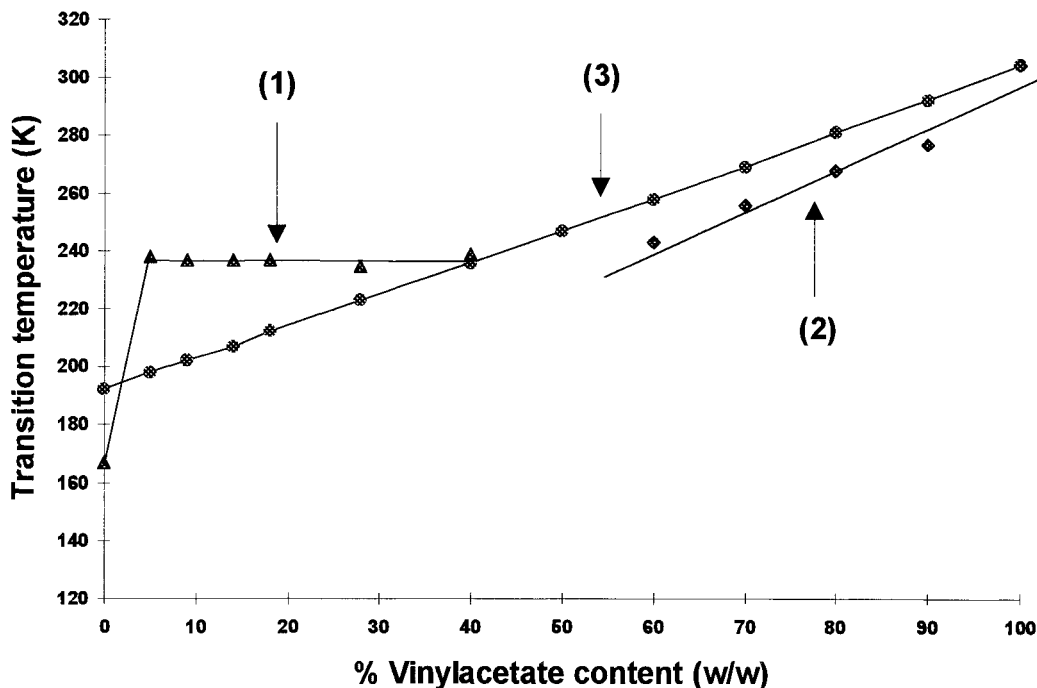


**Figure 8**  $\beta$  transition temperature  $T_\beta$  of EVA A2 oriented amorphous phase versus VA content: (1) our results; (2) the results of Illers<sup>11</sup>; (3) molecular modeling results.

mellae occurs within the copolymer interfacial regions associated with crystallites when the VA content is increased so that the apparent concentration of VA segments into the amorphous phase A2 and then its  $\beta$  transition temperature  $T_\beta$  are almost kept constant. Therefore, both polyethylene and copolymer amorphous phases should be enriched by polyethylene chains arising from the crystalline phase C2 essentially.

However, it has been shown that the crystalline phase C2, which fits copolymer crystallization theories, disappears when the VA content reaches 45 w/w %. Beyond this value, the dilution process should no longer be involved; thus, the  $\beta$  transition temperature  $T_\beta$  disappears because of the absence of amorphous phase A2. A classical glass transition temperature  $T_{g2}$  is recorded and increases continuously with the VA content to reach about 303 K for the pure polyvinylacetate polymer. Taking into account the results obtained by Illers<sup>11</sup> for VA contents ranging from about 60 to 100 w/w %, the increase of the glass transition temperature corresponding to the amorphous copolymer phase of EVA copolymers is actually observed (Fig. 8). Such a variation is consistent with our model. Moreover, we have performed a molecular modeling calculation, based on a connectivity indices algorithm<sup>12</sup> (Biosym software),

of the glass transition temperature in the EVA copolymer for the VA range of 0–100 w/w % (Fig. 8). These calculations suit well the experimental values of the glass transition temperature. Finally, the original phase model proposed in this study clearly explains the nonclassical behaviour of EVA copolymers (5–40 w/w % VA) amorphous phases and confirms that in the range of 5–40 w/w % VA, the well-known theoretical relationships of Gordon and Taylor<sup>13</sup> and Fox<sup>14</sup> do not apply to EVA copolymers.

Moreover, it is important to focus now on the two important assumptions made at the beginning of the study. The first assumption concerns the eventual distribution of compositions in the VA content of the copolymers studied here. We can conclude that even if a composition distribution really exists locally, experimental results concerning amorphous phases, i.e., constancy of  $T_g$  values (Table II) and variations of  $\Delta C_p$  versus average values of VA contents (Fig. 2), remain totally valid. Then, only the idea we have and propose concerning the crystallization behaviour of EVAs could be potentially affected; but it is of major importance to see that either the approaches of Flory (Fig. 3) or Burfield (Fig. 4) fit our experimental results on crystallinity well (the C2 phase, in particular), and that the composition

distribution of EVAs is not a critical parameter. On the other hand, the good agreement observed between the variations of experimental and theoretical curves  $\Delta Cp$  versus mol % VA (Fig. 6), with this theoretical curve being based on average molar fraction of VA comonomers in EVAs, strongly supports our assumption. Concerning the second assumption, i.e., the existence of two predominant crystal morphologies, it is evident that our interpretation of the crystallization behaviour of EVAs allows us to estimate values of melting temperature  $T_f^0$  and melting enthalpy  $\Delta H_{PE}$  for pure polyethylene crystals, as well as of the minimum segmental sequence  $L$  of ethylene entities participating in a crystalline lamellae, which are in very good agreement with data available in the literature. As a conclusion the experimental results obtained strongly confirm our assumptions.

## CONCLUSION

The present study clearly shows that the EVA copolymers are multiphasic materials exhibiting two amorphous phases (polyethylene and EVA) and at least two predominant crystalline phases. When the VA content is increased from 5 to 40 w/w %, the following is observed:

- the  $\beta$  transition temperature of the EVA interlamellar amorphous phase remains constant and disappears when crystallinity does;
- the amount of polyethylene amorphous phase increases;
- the amount of the less-organized crystal structure (involving branched and folded ethylene segmental sequences) remains almost constant; and
- the amount of the slightly branched homostructural polyethylene crystal phase, which suits the general theory of copolymer crystallization, decreases and tends towards zero at a VA content close to 45 w/w %.

Finally, a phase model of EVA copolymers is proposed. All the results can be explained by the fact that when the VA content increases, both amorphous phases are progressively enriched in

polyethylene segments, originating from the well-organized crystalline phase. For VA contents higher than 45 w/w %, when the latter crystalline phase has totally disappeared, no  $\beta$  transition occurs, but a glass transition temperature of the EVA phase is recorded. This latter exhibits classical behaviour and evolution.

Clearly, it is of both fundamental and industrial interest to know, and therefore to control, the nonclassical morphological characteristics of the EVA copolymers in order to adapt their use as adhesive materials. Furthermore, it is expected that relationships between the phase morphology, in particular, in the vicinity of substrate surfaces and the adhesive properties of EVA copolymers, could be established in future work.

The authors wish to thank the Elf-Atochem Company and, particularly, Messrs. R. Panaras, J. C. Robinet, M. Bourrel, and J. Komornicki for financial support and helpful discussions.

## REFERENCES

1. P. J. Flory, *Trans. Faraday. Soc.*, **51**, 848 (1955).
2. D. Burfield, *Macromolecules*, **20**, 3020 (1987).
3. B. Wunderlich, *Data Bank of ATHAS, Advanced Thermal Analysis*, Chem. Dept., University of Tennessee, Knoxville.
4. W. A. Lee and R. A. Rutherford, in *Polymer Handbook*, Vol. III-139, J. Brandrup and E. H. Immergut, Ed., 2nd ed., Wiley, New York, 1975.
5. C. E. Blades, in *Handbook of Adhesives*, I. Skeist, Ed., 2nd ed., Van Nostrand Reinhold, New York, 1977, p. 484.
6. R. F. Boyer, *Macromolecules*, **6**, 288 (1973b).
7. R. Popli and L. Mandelkern, *Polym. Bull.*, **9**, 260 (1983).
8. A. G. Sirota, in *Modifications of Structures and Properties of Polyolefins*, Leningrad, 1974, p. 174.
9. S. L. Aggarval, in *Polymer Handbook*, V-16, J. Brandrup and E. H. Immergut Ed., 2nd ed., Wiley, New York, 1975.
10. L. E. Nielsen, *J. Polym. Sci.*, **42**, 357 (1960).
11. K. H. Illers, *Kolloid Z.*, **190**, 28 (1963).
12. L. B. Kier and L. H. Hall, in *Molecular Connectivity in Structure-Activity Analysis*, Wiley, New York, 1986.
13. M. Gordon and J. S. Taylor, *J. Appl. Chem.*, **2**, 1, (1952).
14. T. G. Fox, *Bull. Am. Phys. Soc.*, **2**, 123 (1956).